Cement & Concrete Composites 34 (2012) 924–930

Contents lists available at SciVerse ScienceDirect

Cement & Concrete Composites

journal homepage: www.elsevier.com/locate/cemconcomp

Carbonation in concrete infrastructure in the context of global climate change – Part 1: Experimental results and model development

S. Talukdar [a,*], N. Banthia [a], J.R. Grace [b]

[a] Department of Civil Engineering, University of British Columbia, Vancouver, Canada
[b] Department of Chemical and Biological Engineering, University of British Columbia, Vancouver, Canada

ARTICLE INFO

Article history:
Received 18 October 2011
Received in revised form 21 April 2012
Accepted 24 April 2012
Available online 15 May 2012

Keywords:
Concrete
Carbonation
Degradation
Modeling
Long term performance

ABSTRACT

There is nearly unanimous consensus amongst scientists that increasing greenhouse gas emissions, including CO_2 generated by human activity, are effecting the Earth's climate. Increasing atmospheric CO_2 emissions will likely increase the rates of carbonation in reinforced concrete structures. However, there is a lack of reliable models to predict the depth of carbonation as a function of time.

To address this deficiency, a numerical model involving simultaneous solution of the transient diffusion and reaction equations of CO_2 and $Ca(OH)_2$ was developed. The model successfully includes the effects of variations in various properties such as porosity, humidity, temperature, atmospheric CO_2 concentrations and chemical reaction rates.

The applicability of the model was confirmed after calibration using data from accelerated carbonation experiments, and the model is used to evaluate the possible effects of climate change by inputting various future climate scenarios in Part 2.

1. Introduction and background

The world's climate is undergoing significant changes, with the effects of these changes expected to be quite profound over the course of this century. The Earth's average temperature has increased by 0.5 °C since the 1970s and is expected to increase by a further 1.4–5.8 °C by the end of this century [1]. Many of the effects of climate change, including temperature change, increase in pollutant concentrations, changes in relative humidity, precipitation, wind patterns, and frequency of severe events (meteorological phenomenon with the potential to cause significant damage, serious social disruption, or loss of human life), could have significant impacts on infrastructure lifespan. Infrastructure capacity could be overwhelmed (rg. dikes failing due to increased sea levels), or it could be degraded (i.e. increased erosion due to extreme weather events). Assessing the impact is difficult, as the relationship between degradation and climate is complex [2]. A concise summary of possible effects of climate change on building materials was provided by Nijland et al. [3].

Limited work has been carried out on the effects that global climate change may have on concrete infrastructure, mainly because the issue has only been recently recognized. Increases in carbonation rates of reinforced concrete structures are expected as a result of increased temperatures and CO_2 concentrations. Two studies in particular are noteworthy. Yoon et al. [4] were the first to consider the effects of climate change on concrete, in particular the effect on carbonation rates. A simplified model was proposed based on a $t^{0.5}$ relationship between time and carbonation depth. While this provides a reasonable approximation, it fails to account for the finite depth and reaction effects. Moreover, this model does not account for the influence of temperature change, which can significantly affect the diffusion coefficient of CO_2 into concrete, the rate of reaction between CO_2 and $Ca(OH)_2$, and the rate of dissolution of CO_2 and $Ca(OH)_2$ in pore water. In addition, the model is a point-in-time predictive model, which assumes CO_2 concentrations to be constant up to a given time, thereby overestimating carbonation depths [5]. Stewart and Ping [5] continued the earlier work by Yoon et al. [4] by taking into account the effect of temperature on the diffusion coefficient, but they did not consider the influence of temperature on the other aforementioned parameters. Their work looked not only at carbonation, but also at the time to crack initiation, crack propagation and failure due to reinforcement corrosion. They also used the same carbonation model as Yoon et al. [4] in their work, but noted that there is a need for an improved model that considers the time-dependent effect of CO_2 concentration and other parameters such as temperature and humidity.

This paper is part of a study being carried out at the University of British Columbia focusing on the effects of global climate change and increasing CO_2 concentrations on the deterioration of reinforced concrete, in particular on rates of carbonation-induced corrosion, with the goal of providing a comprehensive risk assessment

* Corresponding author.
E-mail address: sudip@civil.ubc.ca (S. Talukdar).

0958-9465/$ - see front matter © 2012 Elsevier Ltd. All rights reserved.
http://dx.doi.org/10.1016/j.cemconcomp.2012.04.011

of structural degradation to concrete infrastructure. While the wider study looks at the entire lifespan of a given specimen from initiation of carbonation, to initiation of corrosion, to cracking, spalling, and ultimate failure, the scope of Part 1 of this paper is limited to experimental verification and model development of the carbonation phase of deterioration.

2. Experimental materials and procedure

Tests were performed to accurately measure the carbonation depth under conditions of varying CO_2 concentration, temperature and humidity. To generate these data, concrete specimens were cast, cured, and subjected to accelerated carbonation testing in an ESPEC PR4-KPH carbonation chamber manufactured by ESPEC North America Inc. This chamber was able to electronically control CO_2 concentration, temperature, and relative humidity. Concrete prisms of dimensions 100 mm × 100 mm × 350 mm were cast, allowed to cure in a water bath for 28 days, removed from the bath and then allowed to come to equilibrium with laboratory conditions (20 °C, 60% *RH*) over a further 28 days before being placed in the carbonation chamber. There are currently no standards which specify the drying/conditioning period for carbonation tests. However, based on a review of experimental setups in studies by previous researchers [6–8], it is believed that the conditioning time employed is sufficient to achieve a uniform humidity profile in the concrete cover.

Two types of concrete were tested. One was a virgin, uncontaminated mix, while the other was a chloride-contaminated mix (0.5%/wt. of cement). The contaminated mix was selected to determine whether the presence of chlorides would affect the carbonation progress. For each of the mixes, the slump was maintained at 200 mm and the air content was maintained between 5% and 8%. The mix design is given in Table 1:

Samples were subjected to four different laboratory scenarios, with each scenario running for 8 weeks. The scenarios were selected to evaluate the effect of time for each individual atmospheric variable (CO_2 concentration, temperature and humidity) on carbonation progress. For each type of mix, and for each scenario, five prisms of concrete were cast. This provided a total of 40 prisms cast and subjected to carbonation testing over the course of the study. The scenarios are described in Fig. 1.

For Scenarios B, C and D, Temperature, Relative Humidity, and CO_2 concentration respectively were increased at constant rates over the duration of the scenario. This is mathematically expressed in Table 2. At 7-day intervals, the specimens were removed from the chamber, and sections 30 mm thick were sawcut from each block. Each section was then sprayed with a solution of 1% phenolphthalein in 70% ethyl alcohol. The areas which had been carbonated remained clear in color (pH < 9), whereas uncarbonated areas turned purple (pH > 9). The depth of carbonation could then be determined by averaging the depth along the perimeter of the carbonation front at 12 different locations. A sample section is shown in Fig. 2:

Table 1
Uncontaminated mix design (m^3).

Type 10 portland cement	380 kg
Water	190 kg
Coarse aggregate	800 kg
Fine aggregate	850 kg
Air entrainment Admixture	150 mL

Table 2
Formulas for increases in variables with time.

Scenario B	$T(t) = 25 + (20/56)t$	T: Temperature (C), t: Time (days)
Scenario C	$H(t)=50 + (40/56)t$	H: Relative humidity (%), t: Time (days)
Scenario D	$C(t)=6 + (4/56)t$	C: CO_2 Concentration (%), t: Time (days)

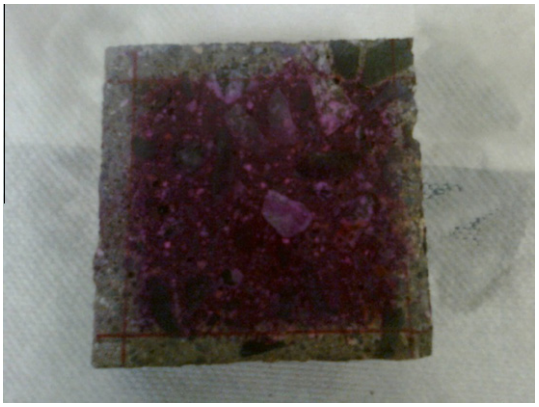

Fig. 2. Carbonated concrete section.

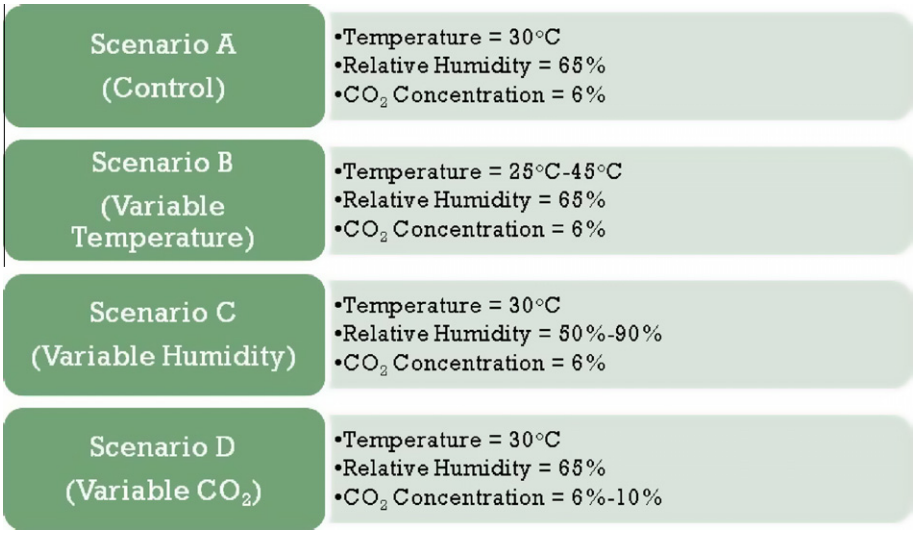

Fig. 1. Laboratory scenarios.

The results of these tests were used to develop the numerical model detailed in Section 3.

3. Model development and verification

3.1. Carbonation reaction

Natural concrete carbonation is a chemical process by which atmospheric CO_2 reacts with $Ca(OH)_2$ to form $CaCO_3$. The reaction predominately used to describe the chemical reaction [9–11] is given in Eq. (1), and a simplified graphic illustrating the reaction in Fig. 3:

$$CO_2 + Ca(OH)_2 \xrightarrow{H_2O} CaCO_3 + H_2O \quad (1)$$

However, in addition to its reaction with $Ca(OH)_2$, CO_2 will also react with C–S–H in concrete to form additional $CaCO_3$ [12–16]. As concrete carbonates, the reaction is fast enough relative to dispersion that two distinct layers can be assumed to form within the concrete. One is the fully carbonated layer into which CO_2 has penetrated and reacted (complete reaction of $Ca(OH)_2$ and C–S–H), and a non-carbonated layer into which CO_2 has not yet penetrated (no reaction of $Ca(OH)_2$ or C–S–H). CO_2 diffuses through the carbonated layer towards the non-carbonated layer.

Park [12] asserted that one-half of carbon dioxide in concrete reacts with $Ca(OH)_2$ while the other half reacts with C–S–H. This assertion was further supported by Glasser and Matschei [17] who showed that the reaction would occur in sequence, with $Ca(OH)_2$ first being fully consumed and then C–S–H, reacting thereby densifying the microstructure. The same was assumed in this study.

Corrosion concerns are augmented when the pH of the concrete drops below 9. This can be detected as described in Section 2. When there are time variations, one-dimensional diffusion of CO_2 into concrete should be modeled assuming non-steady-state diffusion, as per Fick's Second Law. The porosity of the carbonated layer is less than that of the uncarbonated layer, as the volume of carbonation products is greater than that of the non-carbonated concrete. Park [12], found that the pH of concrete drops to ~9 at 50% consumption of $Ca(OH)_2$ in the concrete mix. Therefore, we can determine the location of the carbonation front by modeling to find the location where 50% of the $Ca(OH)_2$ is consumed [12,18].

3.2. Porosity dependence

The intrinsic diffusion rate at which molecules are transported in concrete depends on the size and connectivity of the pore system. As the water/cement (w/c) ratio is lowered, the pore system becomes finer and less connected, leading to lower and lower transport rates and a lower effective diffusivity.

Papadikas et al. [19] proposed an empirical expression to estimate the effective diffusivity of CO_2 in concrete based on its porosity:

$$D_{CO_2} = A\left(\frac{V_p}{\frac{c}{\rho c} + \frac{w}{\rho w}}\right)^u \quad (2)$$

where A and α are empirical parameters determined experimentally with suggested values of $A = 1.64\times10^{-6}$ m^2/s and $\alpha = 1.8$ [19], V_p is the pore volume of cement paste (m^3), c is the cement content (kg), w is the water content (kg), ρ_c is the absolute density of cement (3120 kg/m^3) and ρ_w is the density of water (1000 kg/m^3). Additionally, CO_2 diffusing through concrete will lead to a further reduction in porosity due to carbonation. The expression to account for this further reduction in porosity is found in [19] and is used in the calculation of V_p in Eq. (2). Eq. (2) is used here to estimate the effective diffusivity, subject to modification by other factors, as discussed below.

3.3. Temperature effects

As temperature increases, the diffusivity of gaseous CO_2 increases due to increased molecular activity. The temperature dependence of the diffusion coefficient is commonly assumed [9,20,21] to follow an Arrhenius relationship:

$$D(T) = D_{ref} e^{\left[\frac{Q}{R}\left(\frac{1}{T_{ref}} - \frac{1}{T}\right)\right]} \quad (3)$$

where Q is the diffusion activation energy. The activation energy for CO_2 diffusing in concrete was experimentally determined [21] to be approximately 39,000 J/mol K, R is the gas constant (8.314 J/mol K),

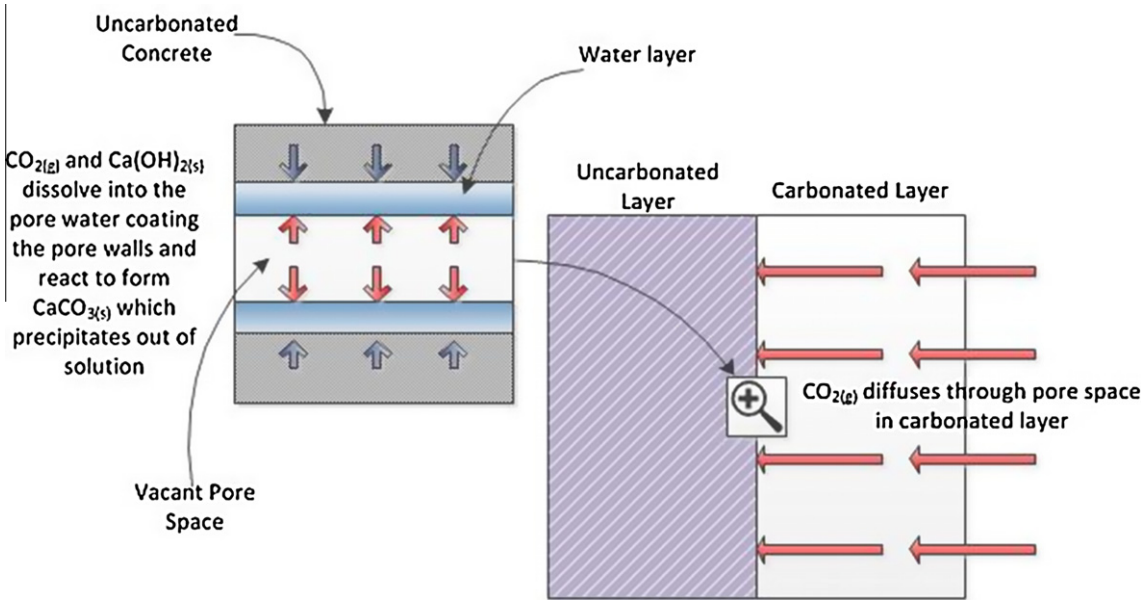

Fig. 3. Carbonation schematic.

T_{ref} is a reference temperature (298 K) and T is the temperature of interest (K). It is also important to determine the rate at which CO_2 reacts with $Ca(OH)_2$ to form $CaCO_3$, as this is also temperature-dependant. Numerous studies have been carried out to determine the reaction rate of CO_2 with $Ca(OH)_2$. Studies [12,19,22,23] have resulted in a wide range of values. Khunthongkeaw and Tangtermsirikul [10] proposed a second order relationship with a rate constant of:

$$K_c = \beta e^{(\frac{-U}{RT})} \tag{4}$$

where k_c is the reaction rate constant for reaction between CO_2 and $Ca(OH)_2$ at the temperature of interest (m^3/mol/s), U is the reaction activation energy (40,000 J/mol K) [10] and β is the pre-exponential factor (1390 m^3/mol/s) [10]. This expression is utilized in the simulations which follow.

3.4. Relative humidity dependence

The moisture content in concrete is of major importance. As CO_2 diffusion controls the carbonation process, the reaction slows down when the pores are water-saturated. In that case, CO_2 hardly reacts with the concrete because of the low rate of diffusion of CO_2 in water. The carbonation reaction also slows down if the concrete is too dry, since, although CO_2 diffuses into the capillary pores, it cannot dissolve into the thin layer of water covering the pores. The higher the humidity, the slower the transport of gaseous CO_2 due to water saturation of pores. The environmental conditions that affect the moisture content in concrete therefore strongly affect carbonation. It has been reported [24] that the optimum climatic conditions for carbonation are a relative humidity between 50% and 70%, with wetting and drying cycles enhancing the reaction.

Papadikas et al. [19], and Saetta et al. [25] expressed the effective diffusivity of CO_2 in concrete taking into consideration humidity, by a function of the form:

$$D \propto (1 - RH)^m \tag{5}$$

where D is the effective diffusivity of CO_2 in concrete, RH is the ambient relative humidity expressed as a fraction, m is a humidity constant, suggested to be $m = 2.2$ [19].

While many researchers agree that the humidity dependence is of this form, different values of m have been proposed, ranging from 0.6 to 2.8 [16,26]. Note that Eq. (5) is only valid for $RH > 0.5$ (50%) as below this value, the pores become too dry, and the reaction is not able to proceed.

3.5. Diffusion of Ca(OH)$_2$

Another factor to consider is the diffusion of dissolved $Ca(OH)_2$ within concrete. However, previous literature indicates that the diffusion of $Ca(OH)_2$ is not as critical as that of CO_2, as it is orders of magnitude smaller than gaseous diffusion. In fact, Papadikas et al. [19] contend that the former may be ignored as it is negligibly small. Park [12] found that the diffusion coefficient of $Ca(OH)_2$ could be maintained at 1×10^{-12} m^2/s and the reaction rate coefficient could be higher by a thousandfold with negligible change in carbonation depth. Therefore, the diffusion coefficient of $Ca(OH)_2$ in this model is taken as 1×10^{-12} m^2/s.

3.6. Formulation of carbonation model

Atmospheric CO_2 diffuses into the concrete primarily through the air space in the pores. The rate of diffusion of CO_2 through the water in the pores is much smaller in magnitude [9], and is therefore ignored.

Upon reaching a given point, gaseous CO_2 dissolves into the water and forms aqueous CO_2 at that location at a concentration governed by Henry's Law:

$$CO_{2(aq)} = HRTCO_{2(g)} \tag{6}$$

where H is Henry's constant (mol/m^3 atm) and R is the gas constant (8.2×10^{-5} m^3 atm/K mol).

Henry's Constant itself varies with temperature [27]:

$$H(T) = H_{ref} e^{[\Delta(\frac{1}{T_{ref}} \frac{1}{T})]} \tag{7}$$

where H_{ref} is the reference Henry's Constant (34.2 mol/m^3 atm) and Δ is an enthalpy constant (2400 K).

CO_2 which has dissolved into the concrete porewater at a given time also reacts with dissolved aqueous $Ca(OH)_2$, to form $CaCO_3$, thereby lowering the overall concentration of CO_2 at that location and time. This is a second order irreversible reaction [10], with its rate given by:

$$r_{CO_2} = K[CO_{2(aq)}][Ca(OH)_{2(aq)}] \tag{8}$$

where k is the reaction rate constant determined by Eq. (4), $CO_{2(aq)}$ and $Ca(OH)_{2(aq)}$ are the aqueous concentrations of carbon dioxide and calcium hydroxide respectively.

There is an upper limit to how much $Ca(OH)_2$ can react, related to the solubility of $Ca(OH)_2$ which can dissolve in the pore water. Unfortunately, there is very limited information on the solubility of $Ca(OH)_2$ in the pores of cement paste/concrete. The only applicable equation for the solubility of $Ca(OH)_2$ in concrete at a given temperature was given [28] as:

$$K_{sp} = (0.0125 \times 10^9) e^{-0.0197} \tag{9}$$

where K_{sp} is the solubility product of Calcium Hydroxide in $mmol^3/l^3$.

Assuming $Ca(OH)_2$ is the predominant alkaline component to dissolve in the pore water, the maximum concentration of $Ca(OH)_{2(aq)}$ in the solution can then be estimated from a basic solubility equilibrium formula:

$$[Ca(OH)_{2(aq)}] = \left(\frac{K_{sp}}{4}\right)^{\frac{1}{3}} \tag{10}$$

Finally, the overall mole balance for CO_2 in concrete pore water at a given location and time is given by the amount of gaseous CO_2 which diffuses into the concrete and then dissolves into the pore water to form $CO_{2(aq)}$ minus the amount of CO_2 which reacts with $Ca(OH)_2$ at that point. If the diffusivity is independent of position, this can be expressed as,

$$\frac{\partial}{\partial t}[CO_{2(aq)}] = D\frac{\partial^2}{\partial x^2}[CO_{2(g)}]HRT - k[CO_{2(aq)}][Ca(OH)_{2(aq)}] \tag{11}$$

for the domain:

$$CO_{2(g)}(x,t) \quad 0 \leqslant x \leqslant L \text{ and } 0 \leqslant t < \infty$$

with initial and boundary conditions:

$$CO_{2(g)}(x,0) = 0 \quad \text{for } x > 0$$

$$CO_{2(g)}(0,t) = CO_{2(atm)}(t) \quad \text{for } t > 0$$

$$\frac{d}{dx}CO_{2(g)}(L,t) = 0 \quad \text{zero-flux boundary}$$

Note that the second condition is a time-dependent boundary condition. Similar to Eq. (11), the mole balance for the overall concentration of $Ca(OH)_2$ in a pore at a given time and location is:

$$\frac{\partial}{\partial t}[Ca(OH)_{2(aq)}] = D\frac{\partial^2}{\partial x^2}[Ca(OH)_{2(aq)}] - k[CO_{2(aq)}][Ca(OH)_{2(aq)}] \tag{12}$$

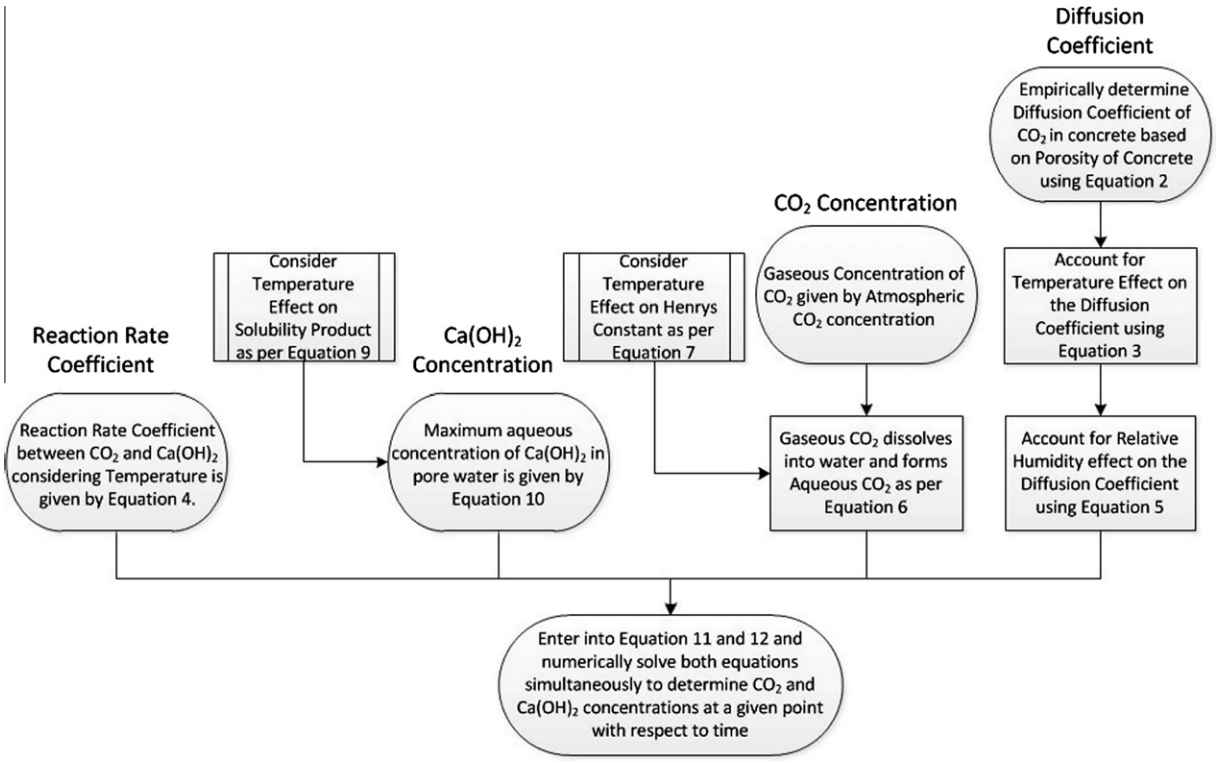

Fig. 4. Flowchart for the determination of CO_2 and $Ca(OH)_2$ concentrations as functions of time.

for the domain:

$$Ca(OH)_{2(aq)}(x,t) \quad 0 \leqslant x \leqslant L \text{ and } 0 \leqslant t < \infty$$

with initial and boundary conditions:

$$Ca(OH)_{2(aq)}(x,0) = Ca(OH)_{2(aq)i} \text{ for } x > 0$$

$$\frac{d}{dx}Ca(OH)_{2(aq)}(0,t) = 0 \quad \text{zero-flux boundary}$$

$$\frac{d}{dx}Ca(OH)_{2(aq)}(0,t) = 0 \quad \text{zero-flux boundary}$$

For concrete, the thermal diffusivity is much greater than the mass diffusivity. Therefore, the temperature of the concrete is assumed to be uniform at any time so that there is no need to also solve the energy equation or to account for the heat of reaction.

A flowchart to illustrate how Eqs. (11) and (12) are formulated is shown in Fig. 4. Eqs. (11) and (12) are solved in MATLAB to determine the concentrations of CO_2 and $Ca(OH)_2$ at a given time and location within a concrete specimen using the *Method of Lines* [29]. They were numerically solved using nodes spaced 5 mm apart in the simulated specimen. The solution turned out to be stiff, and therefore, the 'ODE23s' (2nd/3rd order Runge–Kutta) function was utilized to solve the simultaneous equations, rather than 'ODE45' (4th/5th order Runge–Kutta), the more common solver.

4. Model verification

The results from all four laboratory scenarios were compared with the predictions of the carbonation model as shown in Figs. 5–12.

In order to manually fit the model to the experimental data, the constant A in Eq. (2) was adjusted to 4×10^{-5} m^2/s rather than 1.64×10^{-6} m^2/s as originally proposed [19]. It can be seen from Figs. 5–12 that with the aid of fitting of this single constant, the model matches the experimental results well in six of the eight figures. The fit is less favorable in the cases of Figs. 7 and 8, though the trends are still correct even here. Overall the model can be used to predict carbonation depths in future climate change scenarios. The effect of the presence of chloride ions in the contaminated mixes seems to be negligible, with differences in the rates of carbonation between contaminated and non-contaminated concrete attributable more to differences in air contents.

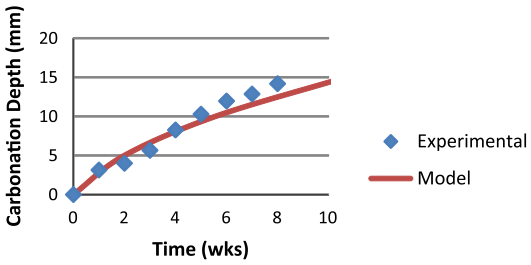

Fig. 5. Comparison of experimental results vs model predictions for scenario A (control), uncontaminated concrete.

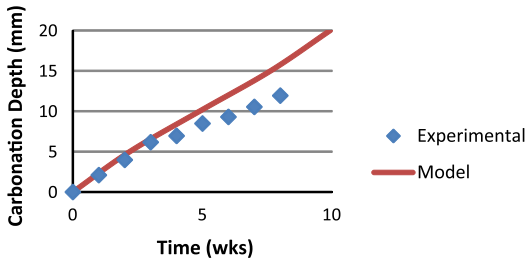

Fig. 6. Comparison of experimental results vs model predictions for scenario B (variable temperature), uncontaminated concrete.

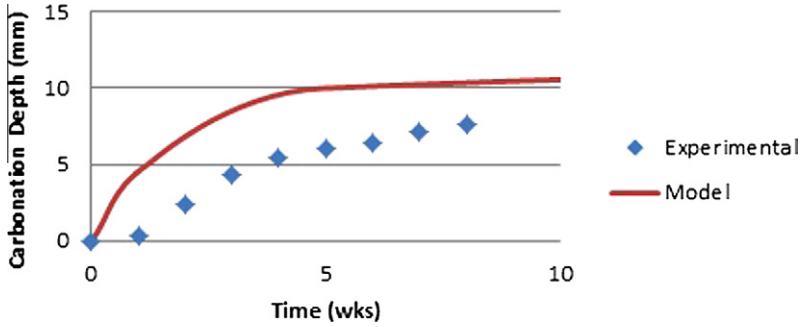

Fig. 7. Comparison of experimental results vs model predictions for scenario C (variable humidity), uncontaminated concrete.

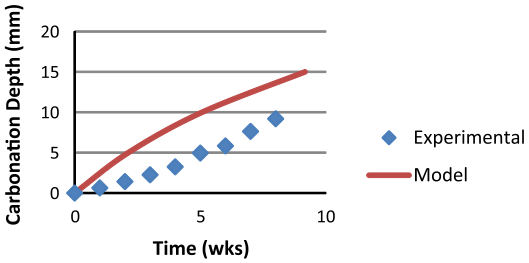

Fig. 8. Comparison of experimental results vs model predictions for scenario D (variable CO_2), uncontaminated concrete.

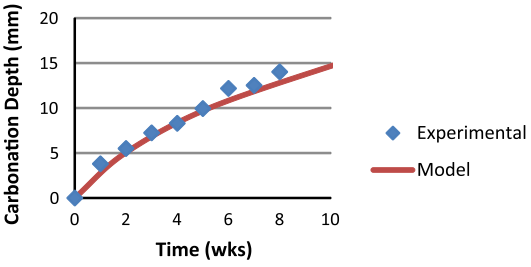

Fig. 9. Comparison of experimental results vs model predictions for scenario A (control), chloride-contaminated concrete.

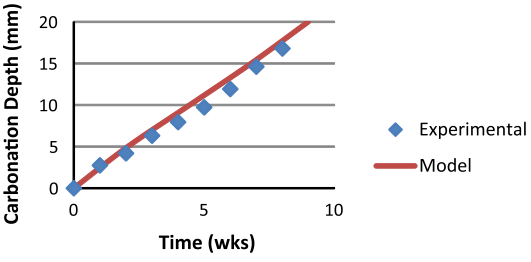

Fig. 10. Comparison of experimental results vs model predictions for scenario B (variable temperature), chloride-contaminated concrete.

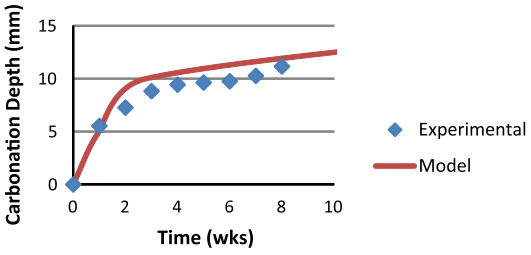

Fig. 11. Comparison of experimental results vs model predictions for scenario C (variable humidity), chloride-contaminated concrete.

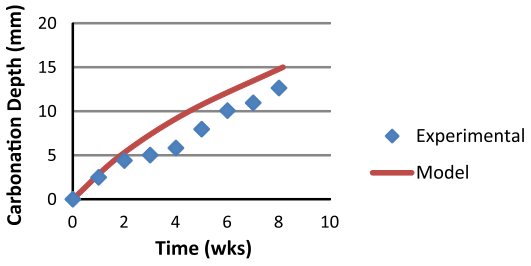

Fig. 12. Comparison of experimental results vs model predictions for scenario D (variable CO_2), chloride-contaminated concrete.

Most carbonation studies use the empirical formulation in Eq. (2) to estimate the effective diffusivity of CO_2 in concrete. However, some studies [13,16] have questioned the value of A originally suggested. Closer examination of Eq. (2) is needed in view of the need to change the value of A in this paper to improve the fit. As the concrete porosity approaches unity, the diffusivity of CO_2 should approach that of the diffusivity of CO_2 in air. A very porous concrete would have a very high water content, and a low cement content. Therefore, in Eq. (2), as c decreases and w increases, V_p, as well as the denominator, approach 1, so that D_{CO2} approaches A. Therefore, A should be close to the value for the diffusivity of CO_2 in air. The diffusivity of CO_2 in air at 298 K has been measured to be 1.65×10^{-5} m^2/s [30], which is much closer to the proposed value of A of 4×10^{-5} m^2/s, rather than 1.64×10^{-6} m^2/s proposed previously [19]. Therefore, for Eq. (2), A should be 4×10^{-5} m^2/s imposing an upper limit on D_{CO2} of 1.65×10^{-5} m^2/s (diffusivity in air).

It has been established that there is a time lag in reaching equilibrium conditions between external and internal relative humidity [6–8], when the external relative humidity is fluctuating. The lag time increases with the depth of concrete, and therefore, the humidity profile is not uniform. For Scenario C where humidity is increased by 40% over 8 weeks, the actual internal relative humidity would likely be less than the external humidity. To rectify this, this scenario could be run over a longer time period to allow internal and external humidities to equilibrate at the carbonation front.

It should be noted that previous studies have found that for natural carbonation of average quality concrete, the measured diffusion coefficient is around $5 \times 10^{-4} - 50 \times 10^{-4}$ cm^2/s [31]. As expected, the simulations for accelerated tests provide a value for the diffusion coefficient that, depending on the scenario, was calculated to be up to 65 times greater than under natural atmospheric

conditions ($1.1 \times 10^{-2} - 3.4 \times 10^{-2}$ cm^2/s). The same code gives diffusion coefficients in the same range as found in [31] for simulations under natural atmospheric conditions (further details are provided in Part 2 of this paper). It is entirely possible that the microstructure of carbonated concrete formed in accelerated conditions may not be the same as under natural conditions. However, considering how well the simulation matches with experimental data, and the reasonable values for the diffusion coefficient obtained under natural conditions, we believe that the results can be applied to simulate natural carbonation as well.

5. Conclusions and future work

A new carbonation model has been developed to predict the depth of carbonation in non-pozzolanic, unloaded concrete specimens, taking into account for the first time, time-varying concentrations of CO_2, temperature and humidity. After fitting, the model was found to predict accelerated carbonation test results quite well. The intention is to use this model to predict the potential effect of future global climate change on reinforced concrete structures.

The next phase of development will be to test the model using variables adjusted simultaneously, rather than one at a time. Secondly, the effect of loading on concrete needs to be examined. It is believed that structures which are cracked or under load will require significantly less time to reach the onset of carbonation-induced corrosion. The ultimate goal is to produce a 'full-life model', which looks at the effects of global climate change on accelerating carbonation-induced corrosion on damaged and undamaged concrete, from initiation, through the propagation phase, to cracking, spalling and ultimate failure.

References

[1] McMichael AJ, Woodruff RE, Hales S. Climate change and human health: present and future risks. Lancet 2006;367:859–69.
[2] Cole IS, Paterson DA. Possible effects of climate change on atmospheric corrosion in Australia. Corros Eng, Sci Technol 2010;45(1):19–26.
[3] Nijland TG, Adan OCG, van Hees RPJ, van Etten BD. Evaluation of the effects of expected climate change on the durability of building materials with suggestions for adaption. Heron 2009;54(1):37–48.
[4] Yoon IS, Copuroglu O, Park KB. Effect of global climatic change on carbonation progress of concrete. Atmos Environ 2007;41(34):7274–85.
[5] Stewart MG, Ping J. Life-cycle cost assessment of climate change adaption measures to minimise carbonation-induced corrosion risks. Int J Eng Under Uncertain: Hazards, Assess Mitigation 2010;2(1–2):35–45.
[6] Russell D, Basheer PAM, Rankin GIB, Long AE. Effect of relative humidity and air permeability on prediction of the rate of carbonation of concrete. Struct Build 2001;146(3):319–26.
[7] Franzen C, Mirwald PW. Moisture content of natural stone: static and dynamic equilibrium with atmospheric humidity. Environ Geol 2004;46(3–4):391–401.
[8] Ryu DW, Ko JW, Noguchi T. Effects of simulated environmental conditions on the internal relative humidity and relative moisture content distribution of exposed concrete. Cem Concr Compos 2011;33(1):142–53.
[9] Saetta AV, Schrefler BA, Vitaliani RV. The carbonation of concrete and the mechanism of moisture, heat and carbon dioxide flow through porous materials. Cem Concr Res 1993;23(4):761–72.
[10] Khunthongkeaw J, Tangtermsirikul S. Model for simulating carbonation of fly ash concrete. J Mater Civ Eng 2005;17(5):570–8.
[11] Isgor OB, Razaqpur AG. Finite element modeling of coupled heat transfer, moisture transport and carbonation processes in concrete structures. Cem Concr Compos 2004;26(1):57–73.
[12] Park DC. Carbonation of concrete in relation to CO_2 permeability and degradation of coatings. Constr Build Mater 2008;22(11):2260–8.
[13] Wang XY, Lee HS. A model predicting carbonation depth of concrete containing silica fume. Mater Struct 2009;42(6):691–704.
[14] Peter MA, Muntean A, Meier Bohm M. Competition of several carbonation reactions in concrete: a parametric study. Cem Concr Res 2008;38(12):1385–93.
[15] Borges PHR, Costa JO, Milestone NB, Lynsdale CJ, Streatfield RE. Carbonation of CH and CSH in composite cement pastes containing high amounts of BFS. Cem Concr Res 2010;40(2):284–92.
[16] Bahador SB, Cahyadi JH. Modelling of carbonation of PC and blended cement concrete. The IES J Part A: Civil Struct Eng 2009;2(1):59–67.
[17] Glasser FP, Matschei T. Interactions between portland cement and carbon dioxide. In: Proceedings of the 12th ICCC. Montreal, Canada; 2007.
[18] Chang CF, Chen JW. The experimental investigation of concrete carbonation depth. Cem Concr Res 2006;36(9):1760–7.
[19] Papadakis VG, Vayenas CG, Fardis MN. Physical and chemical characteristics affecting the durability of concrete. ACI Mater J 1991;8(2):186–95.
[20] Song HW, Kwon SJ, Byon KJ, Park CK. Predicting carbonation in early-aged cracked concrete. Cem Concr Res 2006;36(5):979–89.
[21] Saeki T, Ohga H, Nagataki S. Mechanism of carbonation and prediction of carbonation process of concrete. Concr Libr JSCE 1991;17:23–6.
[22] Van Balen K, Van Gemert D. Modelling lime mortar carbonation. Mater Struct 1994;27(7):393–8.
[23] Ishida T, Maekawa K. Modeling of pH Profile in pore water based on mass transport and chemical equilibrium theory. Proc JSCE 2000;648(47).
[24] Marie-Victoire E, Cailleux E, Texier A. Carbonation and historical buildings made of concrete. J Phys IV 2006;136(2006):305–18.
[25] Saetta AV, Schrefler BA, Vitaliani RV. 2-D model for carbonation and moisture/heat flow in porous materials. Cem Concr Res 1995;25(8):1703–12.
[26] Ceukelaire D, Van Nieuwenburg D. Accelerated carbonation of a blast-furnace cement concrete. Cem Concr Res 1993;23(2):442–52.
[27] Fogg PGT, Sangster J. Chemicals in the atmosphere: solubility, sources and reactivity. West Sussex: John Wiley & Sons Ltd; 2003.
[28] Nakarai K, Ishida T, Maekawa K. Modeling of calcium leaching from cement hydrates coupled with micro-pore formation. J Adv Concr Technol 2006;4(3):395–407.
[29] Cutlip MB, Shacham M. Problem solving in chemical and biochemical engineering with polymath, excel, and matlab. 2nd ed. Upper Saddle River: Prentice-Hill; 2007.
[30] Marrero TR, Mason MA. Gaseous diffusion coefficients. J Phys Chem Ref Data 1972;1:3–118.
[31] Sanjuan MA, del Olmo C. Carbonation resistance of one industrial mortar used as a concrete coating. Build Environ 2001;36(8):949–53.